



Article

# Automatic Diagnosis of Chronic Thromboembolic Pulmonary Hypertension Based on Volumetric Data from SPECT Ventilation and Perfusion Images

Alexander P. Seiffert <sup>1,\*</sup> , Adolfo Gómez-Grande <sup>2</sup>, Patrick Pilkington <sup>2</sup>, Paula Cara <sup>1</sup>, Héctor Bueno <sup>3,4,5,6</sup> , Juana Estenoz <sup>2</sup>, Enrique J. Gómez <sup>1,7</sup> and Patricia Sánchez-González <sup>1,7,\*</sup>

<sup>1</sup> Biomedical Engineering and Telemedicine Centre, ETSI Telecomunicación, Center for Biomedical Technology, Universidad Politécnica de Madrid, Madrid 28040, Spain; paula.cara@alumnos.upm.es (P.C.); enriquejavier.gomez@upm.es (E.J.G.)

<sup>2</sup> Department of Nuclear Medicine, Hospital Universitario 12 de Octubre, Madrid 28041, Spain; adolfo.gomez@salud.madrid.org (A.G.-G.); johnpatrick.pilkington@salud.madrid.org (P.P.); juanamarca.estenoz@salud.madrid.org (J.E.)

<sup>3</sup> Department of Cardiology and Instituto de Investigación Sanitaria (imas12), Hospital Universitario 12 de Octubre, Madrid 28041, Spain; hector.bueno@cnic.es

<sup>4</sup> Centro Nacional de Investigaciones Cardiovasculares (CNIC), Madrid 28029, Spain

<sup>5</sup> Faculty of Medicine, Universidad Complutense de Madrid, Madrid, 28040, Spain

<sup>6</sup> Centro de Investigación Biomédica en Red de Enfermedades Cardiovasculares (CIBERCV), Madrid 28029, Spain

<sup>7</sup> Centro de Investigación Biomédica en Red de Bioingeniería, Biomateriales y Nanomedicina (CIBER-BBN), Madrid 28029, Spain

\* Correspondence: ap.seiffert@upm.es (A.P.S.); p.sanchez@upm.es (P.S.-G.)

Received: 14 July 2020; Accepted: 31 July 2020; Published: 3 August 2020



**Abstract:** Chronic thromboembolic pulmonary hypertension (CTEPH) is confirmed by visual analysis of single-photon emission computer tomography (SPECT) ventilation and perfusion (V/Q) images. Defects in the perfusion image discordant with the ventilation image indicate obstructed segments and the positive diagnosis of CTEPH. A quantitative metric and classification algorithm are proposed based on volumetric data from SPECT V/Q images. The difference in ventilation and perfusion volumes ( $V_{V-P}$ ) is defined as a quantitative metric to identify discordant defects in the SPECT images. The algorithm was validated with 22 patients grouped according to their diagnosis: (1) CTEPH and (2) respiratory pathology. Volumetric data from SPECT perfusion images was also compared before and after treatment for CTEPH. CTEPH was detected with a sensitivity of 0.67 and specificity of 0.80. The performance of volumetric data from SPECT perfusion images for the evaluation of treatment response was studied for two cases and improvement of pulmonary perfusion was observed in one case. This study uses volumetric data from SPECT V/Q images for the diagnosis of CTEPH and its differentiation from respiratory pathologies. The results indicate that the defined metric is a viable option for a quantitative analysis of SPECT V/Q images.

**Keywords:** CTEPH; pulmonary hypertension; SPECT V/Q; quantification; segmentation; computer-assisted diagnosis; treatment response

## 1. Introduction

Pulmonary hypertension (PH) describes a group of pathologies that are defined by an increase of the mean pulmonary arterial pressure (PAP) greater than 25 mmHg at rest [1]. Due to the increase in PAP, right cardiac overload is induced and the cardiac muscle is weakened, resulting in right ventricular pressure dysfunction [1,2].

Chronic thromboembolic pulmonary hypertension (CTEPH) is a severe variant of PH. It is caused by the occlusion of pulmonary arteries and arterioles by organized blood clots. This results in obstructed segments in the pulmonary perfusion [3]. CTEPH occurs due to pulmonary thromboemboli and can appear after acute pulmonary embolism (PE); however, it is considered rare [4,5].

The initial diagnosis is usually performed with a qualitative scale and confirmed by medical imaging. Single-photon emission computer tomography (SPECT) ventilation and perfusion (V/Q) images are visually analyzed. As CTEPH is defined by the obstruction of the pulmonary perfusion, the corresponding SPECT perfusion image reveals defects of triangular morphology. However, while these defects are visible in the perfusion image, they are absent in the ventilation image. The presence of discordant defects in the perfusion image confirms the diagnosis of CTEPH [6]. The following criteria are defined for the visual analysis [3]:

- Positive CTEPH diagnosis—presence of at least one segmental defect or two subsegmental perfusion defects not consistent with ventilation in pulmonary SPECT images.
- Negative CTEPH diagnosis—normal perfusion in which the edges of the lung are preserved or presence of concordant defects in both the ventilation and perfusion images.
- Respiratory pathology—presence of defects in the ventilation image that are not concordant with the perfusion.

Moreover, CTEPH is the only cause of severe PH that can be treated surgically without the need for lung transplantation. The most common treatment for severe CTEPH is pulmonary thromboendarterectomy. This surgical procedure involves the removal of thromboembolic material that occludes the pulmonary arteries, resulting in significant improvements in hemodynamic and right ventricular function [7]. Alternatives to endarterectomy for those patients with recurrent CTEPH, who are inoperable, or those in whom the risk–benefit ratio of pulmonary endarterectomy is unacceptable, are balloon pulmonary angioplasty [8] or anticoagulant and vasodilator pharmacological treatments, which help to dissolve the thrombus and prevent its recurrence [9]. After the treatment, the blood flow to the problematic segments should be regained, resulting in the disappearance of the hypoperfused regions in the SPECT perfusion image.

The ventilation and perfusion of the lungs on SPECT V/Q images for the diagnosis and evaluation of treatment response of CTEPH is usually based on a qualitative analysis of the image data. SPECT V/Q is also used as a reference in the evaluation of other diagnostic techniques [10–16]. The quantitative analysis of lung perfusion on SPECT images by volumetric data has previously been proposed [17]. In the study, lung perfusion volume on SPECT images was segmented by thresholding and compared to anatomical lung volume, as well as clinical parameters, showing the feasibility of quantitative analysis of SPECT perfusion scans. Based on the guidelines and criteria defined for the diagnosis of CTEPH in SPECT V/Q images, as well as the qualitative analysis of those images presented in the cited studies, it can be assumed that functional volumetric data could aid in the diagnostic process. Given the presence of reduced perfusion compared to ventilation, the difference between both volumes is evaluated as a quantitative parameter for the diagnosis of CTEPH.

A new quantitative metric based on volumetric data from SPECT V/Q images is proposed in this study. A quantitative scale based on reference values was designed and validated to automatically classify patients into CTEPH or presenting a respiratory pathology. The defined algorithm also takes into account the guidelines for visual inspection of SPECT V/Q images defined by the European Association of Nuclear Medicine (EANM) [3] and the European Society of Cardiology (ESC)/European Respiratory Society (ERS) [6]. Lastly, the utility of volumetric measurements from SPECT perfusion images for the evaluation of treatment response in CTEPH was assessed.

## 2. Materials and Methods

### 2.1. Patients

All patients who were hospitalized between June 2017 and May 2019 in the *Hospital Universitario 12 de Octubre*, Madrid, Spain, with suspected CTEPH as an initial diagnosis, were included in the study group. Additional inclusion criteria were:

- Suspicion of CTEPH as an initial diagnosis at first appearance, after remitting for symptoms such as chest pain and dyspnea;
- Availability of SPECT V/Q images;
- Confirmation of diagnosis of old CTEPH with or without recent improvement in pulmonary perfusion.

The exclusion criteria before defining the final database were:

- SPECT V/Q study with artifacts;
- Inconclusive or indeterminate studies;
- Visually identifiable extensive radiotracer accumulations in specific regions of the pulmonary parenchyma during the ventilation study, caused by the presence of excess mucus.

Lastly, if any of the selected cases of the CTEPH group underwent treatment with available SPECT V/Q images, they were included in the study group. These cases were analyzed separately to study the usefulness of the proposed quantification in the evaluation of the treatment response.

### 2.2. Image Acquisition

SPECT V/Q images were acquired using a SKYLIGHT gamma camera (Philips, Amsterdam, Netherlands) with a low energy all-purpose (LEAP) collimator. During the 360° circular rotation of the gamma camera in “step and shoot” mode, 64 projections were acquired, each with a duration of 30 s. Ventilation studies were performed after the administration via airway of <sup>99m</sup>Tc-Technegas. The aerosol was inhaled by the patients for 15–20 min through deep, slow breaths with 5 second pauses between each breath. For the pulmonary perfusion study, 185 MBq of technetium macroaggregated albumin (<sup>99m</sup>Tc-MAA) was administered intravenously. The images had a matrix size of 64 × 64 and were processed at a JETStream Workspace version 3.0 (Philips, Amsterdam, The Netherlands) workstation.

### 2.3. Image Analysis

SPECT images were analyzed using MATLAB R2018b (The MathWorks, Inc., Natick, Massachusetts, USA). All analyses were performed for each lung separately due to the anatomical differences between the left and right lung [18].

As mentioned above, discordant defects between ventilation and perfusion images indicate CTEPH or other respiratory pathologies. The difference between the ventilation and perfusion volumes ( $V_{V-P}$ ) is proposed as a novel quantitative metric for the diagnosis of CTEPH and the differentiation from respiratory pathologies. Thus, large differences of the individual volumes indicate possible CTEPH or a respiratory pathology. The ventilation and perfusion volumes ( $V_V$  and  $V_P$ , respectively) were extracted based on threshold segmentation. The threshold was defined as a percentage of the maximum voxel intensity of the analyzed image. The percentage used is hereafter referred to as “threshold”. The optimal segmentation thresholds were defined using the images of the reference group. Moreover, the degree of discordance was evaluated based on values of  $V_{V-P}$  obtained from this group. Therefore, the image analysis was divided into three steps: (1) calculation of reference values, (2) definition of diagnostic margins, and (3) application in pathological cases that correspond to the second and third group of the patient database to validate the algorithm. The methodology is shown in Figure 1.

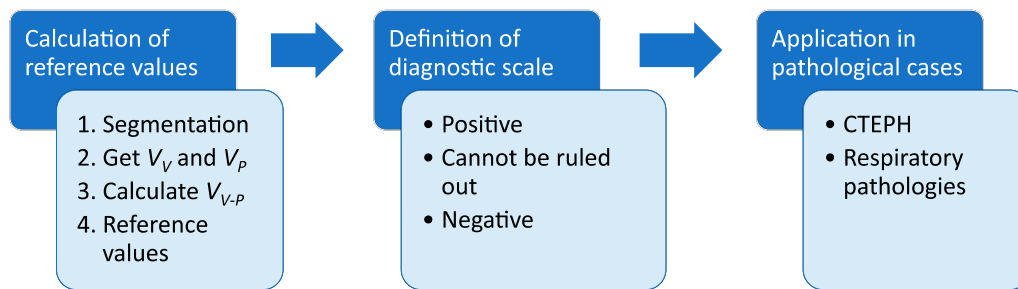


**Figure 1.** Methodology (CTEPH, chronic thromboembolic pulmonary hypertension).

### 2.3.1. Calculation of Reference Values

To obtain reference values of normal or concordant lung volumes, at first the images of the reference group were analyzed. A total of four reference values per lung were calculated based on the images. These were:

- Optimal segmentation thresholds for the ventilation images;
- Optimal segmentation thresholds for the perfusion images;
- Mean average  $V_{V-P}$  among all patients of the reference group ( $Mean(V_{V-P, ref})$ ) for all evaluated pairs of segmentation thresholds;
- Minimum average  $V_{V-P}$  among all patients of the reference group ( $Min(V_{V-P, ref})$ ) for all evaluated pairs of segmentation thresholds.

First, the images were iteratively segmented with different thresholds defined between two initial values and increasing the percentage by 1. These initial thresholds of the grid search were obtained by visually identifying those values when regions were included in the segmentation that do not belong to the lung (for the superior threshold) or when not the entire lung was segmented (for the inferior threshold). Then,  $V_V$  and  $V_P$  were obtained for each pair of thresholds (one for the ventilation image and another for the perfusion image) and each case of the reference group. It must be noted that the volumes obtained from cases without defects or presenting concordant defects were not the same. Therefore, the mean  $V_{V-P}$  was calculated for each pair of thresholds among all patients of the reference group. Lastly, the average of these mean  $V_{V-P}$  values was defined as the  $Mean(V_{V-P, ref})$ . The lowest average  $V_{V-P}$  ( $Min(V_{V-P, ref})$ ) among all patients of the reference group out of the evaluated pairs of segmentation thresholds was also calculated. Its corresponding thresholds were then established as the optimal segmentation thresholds for the ventilation and perfusion images.

### 2.3.2. Definition of Diagnostic Scale

To classify pathological cases, a diagnostic scale based on the reference values was defined. These reference values were used as cut-off values to confirm or refuse the diagnosis of CTEPH. Given that even those cases without defects or with concordant defects do not present the same lung volumes, the degree of the difference compared to a reference group was taken into account when identifying pathological cases. Moreover, and previously to applying this quantitative scale, the sign of  $V_{V-P}$  needs to be evaluated. When  $V_{V-P}$  is positive,  $V_V$  is greater than  $V_P$  and the defects are present in the perfusion image and correspond to a CTEPH pattern. On the contrary, when  $V_{V-P}$  is negative,  $V_P$  is greater than  $V_V$  and the defects are present in the ventilation image, indicative of a respiratory pathology. Afterwards, the absolute value of  $V_{V-P}$  is compared to the reference values and a diagnosis is established following the conditions defined in Table 1.

**Table 1.** Definition of the quantitative diagnostic scale.

Diagnosis	Cut-Off Values
Positive	$ V_{V-P}  > Mean(V_{V-P, ref})$
Cannot be ruled out	$Mean(V_{V-P, ref}) \geq  V_{V-P}  \geq Min(V_{V-P, ref})$
Negative	$ V_{V-P}  < Min(V_{V-P, ref})$

### 2.3.3. Application in Pathological Cases

The validation of the proposed metric and quantitative diagnostic scale was carried out by applying the algorithm to the cases of the second (CTEPH) and third (respiratory pathologies) group. The ventilation and perfusion volumes were extracted based on the previously defined optimal segmentation thresholds and their difference was calculated. Following the scale shown in Table 1, each case was automatically classified based on its  $V_{V-P}$ :

- Volume difference values between ventilation and perfusion, which were above the  $Mean(V_{V-P, ref})$  value, indicated a positive diagnosis;
- Volume difference values between ventilation and perfusion, which were below the  $Mean(V_{V-P, ref})$  value and above the  $Min(V_{V-P, ref})$  value, indicated suspicion of CTEPH or respiratory pathology, whose diagnosis could not be ruled out, but required a complementary visual analysis to confirm the positive diagnosis of either CTEPH or a respiratory pathology;
- Volume difference values between ventilation and perfusion, which were below the  $Min(V_{V-P, ref})$  value, indicated a negative diagnosis.

To evaluate the accuracy of the algorithm, a 3-class confusion matrix was generated and the overall accuracy, as well as the sensitivity and specificity of each class were calculated. A case was considered correctly classified if the algorithm confirmed or could not rule out a positive diagnosis in one of the two lungs of the patients.

Finally, the volumetric analysis of SPECT images was applied to the evaluation of treatment response in CTEPH. Given that the treatment aims to correct the obstructed segments and improve perfusion, the volume after the treatment ( $V_{post}$ ) should be higher than before ( $V_{pre}$ ). Therefore, the difference of perfusion volumes ( $V_{post-pre}$ ) was calculated and compared to the patients' response.

## 3. Results

### 3.1. Study Group

The final study group after applying the inclusion and exclusion criteria defined in the methodology was composed of 32 patients. These were divided into three groups according to the diagnosis established by specialists in nuclear medicine of the hospital. The demographic characteristics of the patients of each group are shown in Table 2.

**Table 2.** Demographics of the study population (m, male; f, female; y, years; SD, standard deviation).

	N	Gender (m/f)	Age (y ± SD)
Reference	10	2/8	61.40 ± 9.74
CTEPH	12	8/4	61.50 ± 13.44
Respiratory pathology	10	2/8	70.10 ± 13.51
Total	32	12/20	64.16 ± 12.82

Resuming, the reference group was composed of 10 patients who did not show any nonconcordant defect in the pulmonary SPECT V/Q images, so they were assumed as patients with normal lung function or patients with concordant defects in both images. The diagnosis of CTEPH was confirmed in 12 patients. The 10 patients that composed the third group were diagnosed with a respiratory

pathology including chronic obstructive pulmonary disease (COPD) and chronic bronchitis, or some type of PH without thromboembolism.

Within the CTEPH group, two patients underwent treatment and perfusion SPECT images before and after the treatment are available. These two patients were a 55-year-old woman and a 64-year-old man.

### 3.2. Calculation of Reference Values

After the visual analysis of the results of different segmentation thresholds, the upper and lower values of the grid search were determined. Concretely, the grid search was performed between 14% and 22% and increasing the segmentation thresholds by 1% in each iteration. The optimal segmentation thresholds for the ventilation and perfusion images and for each lung are shown in Table 3. The table also includes the reference values of volume differences. These correspond to the segmentation of the images of the reference group using the pairs of segmentation thresholds shown in the same table.

**Table 3.** Optimal segmentation thresholds and reference values of volume difference.

	Left Lung	Right Lung
Ventilation	21%	15%
Perfusion	18%	21%
$Mean(V_{V-P, ref})$	816.04 cm <sup>3</sup>	328.82 cm <sup>3</sup>
$Min(V_{V-P, ref})$	466.84 cm <sup>3</sup>	119.01 cm <sup>3</sup>

An example of the segmented SPECT ventilation and perfusion images is shown in Figure 2. These correspond to a 58-year-old woman of the reference group who presents normal lung function. Both images show relative homogeneous uptake patterns. The complete lung volume was segmented in both images and visually they are similar. The difference between ventilation and perfusion volumes in both lungs was less than 200 cm<sup>3</sup>.

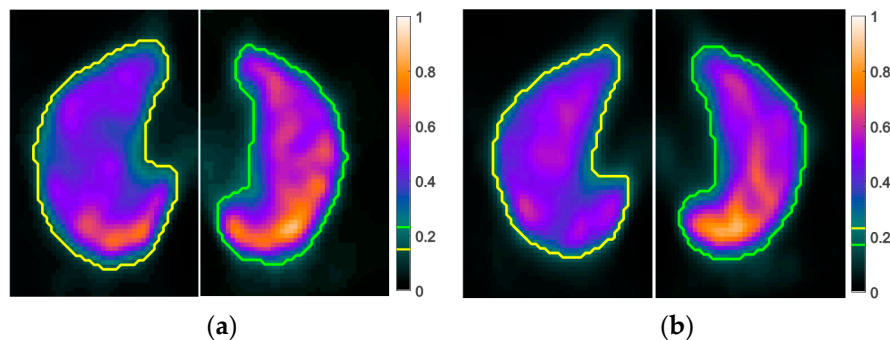


**Figure 2.** Segmented single-photon emission computer tomography (SPECT) images of a reference group patient. The contour of the segmentation is drawn in yellow (right lung) and green (left lung) in the images and the color bar: (a) ventilation, (b) perfusion.

### 3.3. Definition of Diagnostic Scale

After obtaining the reference volumes, these were applied to define the final quantitative diagnostic scale (see Table 4) that was described in the previous section. To determine if the case was a potential CTEPH or respiratory pathology, the sign of  $V_{V-P}$  was first evaluated, and afterwards its absolute value was used.



**Table 4.** Quantitative diagnostic scale.

Diagnosis	Left Lung	Right Lung
Positive	$ V_{V-P}  > 816.04 \text{ cm}^3$	$ V_{V-P}  > 328.82 \text{ cm}^3$
Cannot be ruled out	$816.04 \text{ cm}^3 \geq  V_{V-P}  \geq 466.84 \text{ cm}^3$	$328.82 \text{ cm}^3 \geq  V_{V-P}  \geq 119.01 \text{ cm}^3$
Negative	$ V_{V-P}  < 466.84 \text{ cm}^3$	$ V_{V-P}  < 119.01 \text{ cm}^3$

**3.4. Application in Pathological Cases**

The optimal segmentation thresholds shown in Table 3 were used to obtain the values of  $V_{V-P}$  for each patient of groups two and three, that is, patients that present discordant defects in the images. With these values, the diagnosis was determined by the algorithm for each lung separately based on the conditions defined in Table 4. Examples of patients with either CTEPH or a respiratory pathology are shown in Figure 3. The case of CTEPH corresponds to a 64-year-old man. A region of hypoperfusion with the typical triangular morphology can be identified in the perfusion image. Due to the lower uptake, these regions were not segmented by the algorithm as the voxel values are beneath the segmentation threshold. The second case corresponds to a 63-year-old woman diagnosed with chronic obstructive pulmonary disease. A hypoventilated region can be identified in the ventilation image and no defects are present in the perfusion image. These regions were not segmented, as can be seen by the drawn contour.

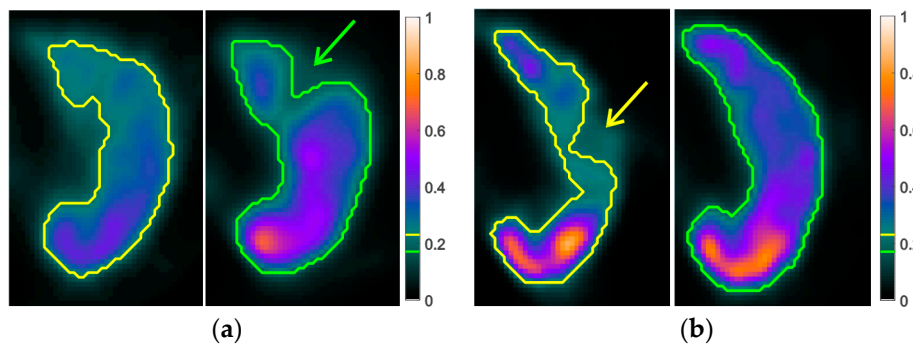


**Figure 3.** Segmented SPECT ventilation (left) and perfusion (right) images of a left lung. The contour of the segmentation is drawn in yellow (ventilation) and green (perfusion) in the images and the color bar. (a) Patient with CTEPH and typical perfusion defects (arrow). (b) Patient with a respiratory pathology and typical ventilation defect (arrow).

After processing all images, the cases of each group were classified into CTEPH, respiratory pathology, or none. As is mentioned in the methodology, a case was classified correctly if the algorithm returned a “positive” or “cannot be ruled out” verdict for one of the two lungs. The overall accuracy of the algorithm, determined from the 3-class confusion matrix, was 0.64. In the CTEPH group, 8 of 12 patients were correctly classified. On the other hand, 6 of 10 patients with a respiratory pathology were correctly classified. The sensitivity and specificity of each class is shown in Table 5.

**Table 5.** Classification results.

	CTEPH	Respiratory Pathology
Accuracy	0.67	0.60
Sensitivity	0.67	0.60
Specificity	0.80	0.92

Regarding the treatment response to CTEPH,  $V_{pre}$  and  $V_{post}$  were obtained and the difference was calculated. The optimal segmentation thresholds for the perfusion image were used to calculate the perfusion volumes. The perfusion SPECT images before and after treatment for patients 1 and 2 are

shown in Figure 4. An improvement can be observed in the images after the treatment for patient 1. Patient 2 shows no improvement of the segmented perfusion volume after the treatment for CTEPH. This improvement, or lack of improvement, can also be observed in the quantitative values shown in Table 6.

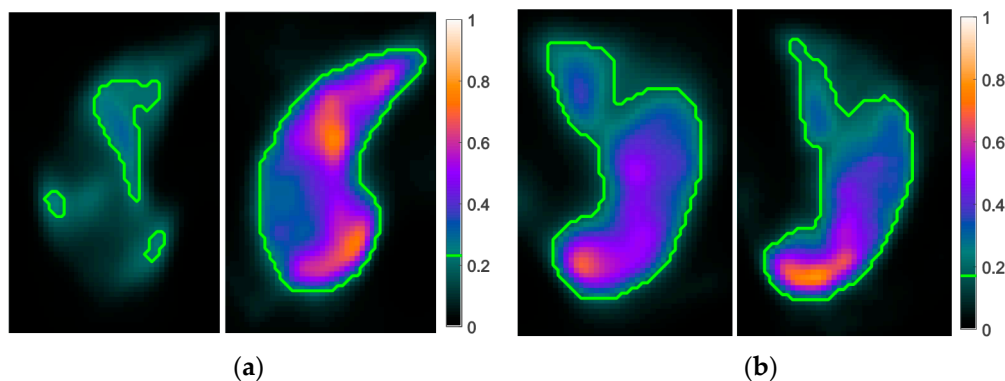


**Figure 4.** Perfusion SPECT images pre-treatment (left) and post-treatment (right). The contour of the segmentation is drawn in green in the images and the color bar. (a) Patient 1 (right lung). (b) Patient 2 (left lung).

**Table 6.** Perfusion volumes before and after treatment for CTEPH.

	Patient 1		Patient 2	
	Left Lung	Right Lung	Left Lung	Right Lung
$V_{pre}$ (cm <sup>3</sup> )	443.04	335.41	1075.04	2924.69
$V_{post}$ (cm <sup>3</sup> )	999.44	1488.33	612.37	1112.32
$V_{post-pre}$ (cm <sup>3</sup> )	556.40	1152.93	−43.04	−1812.36
Improvement (%)	12.57	77.46	No improvement	No improvement

#### 4. Discussion

In this study, a novel quantitative metric obtained from SPECT V/Q images is proposed for the diagnosis of CTEPH. The metric is based on the volumetric data obtained from SPECT images that were shown to be more sensitive than planar imaging for detecting obstructed segments due to CTEPH [19].

To obtain the optimal segmentation thresholds for the ventilation and perfusion volumes of the SPECT images, a reference group was defined composed of cases without discordant defects in the pulmonary SPECT images. It is important to bear in mind that the reference group was composed of eight women and two men. Therefore, the optimal segmentation thresholds and  $V_{V-P}$  reference values were more representative of a female population. This gender imbalance had a great influence on the overall classification results of the patients of the second and third group. This can be explained by the anatomical differences between female and male lungs, as the former are generally smaller [20]. Concretely, the algorithm overestimated possible defects in men because obstructed segments of the same anatomical extent in both genders tend to be greater in men and thus, the difference between ventilation and perfusion volumes was higher. Moreover, the difference needed to be much higher in women to receive a positive diagnosis. This can be observed in the results and gender distribution after applying the obtained reference values to the patients diagnosed with CTEPH or a respiratory pathology.

In the case of the patients diagnosed with CTEPH, 6 of the 12 cases were classified as “positive” and 2 yielded a “cannot be ruled out” result. Regarding the gender distribution, 5 of the 8 men were correctly classified and the positive diagnosis could not be ruled out for an additional case. It is also noteworthy that only one of the patients classified as positive with certainty was a woman. Out of the three other women, for one a positive diagnosis could not be ruled out and two received a negative



diagnosis. As can be seen by this distribution, most correctly classified cases corresponded to the male patients.

The same pattern can be observed when analyzing the results of the cases diagnosed with respiratory pathologies. Both men who were included in this group were correctly diagnosed with a respiratory pathology. All cases that received a negative diagnosis corresponded to female patients. Moreover, in two cases, the algorithm detected a larger ventilation volume than perfusion volume, which indicates a possible CTEPH and not a respiratory pathology.

In addition to the gender imbalance of the reference group, both groups used for the validation were also not composed equally of women and men. This led to the relatively low sensitivity values, due to the aforementioned overestimation of defects in male patients. Therefore, it can be stated that the main limitation of this study was the composition of the study groups. Not only were they heterogeneous regarding the gender of the patients, but the reference group also consisted of only 10 patients, which included cases of normal lung function and concordant defects present in the SPECT images. To improve the preliminary results presented in this study, the algorithm should be applied separately to women and men. Thus, the segmentation thresholds and reference values for the classification would be gender specific and it can be assumed that the results improve. Another limitation, related to the selected study group, was the exclusion of cases with extensively accumulated radiotracer in the SPECT images. However, less extensive accumulations were still present in some studies and would affect the algorithm. Therefore, an image preprocessing algorithm should be implemented to be able to include these cases and improve the overall performance of the algorithm.

Moreover, in this study, only two cases were available for the comparison of the perfusion volumes before and after the treatment. In addition, similar to the previous cases, the segmentation thresholds need to be reevaluated. Moreover, volumetric measurements were only partially useful when evaluating treatment response, as it offers no spatial information. While a general improvement could be determined when the perfusion volume increases, the same could not be said when the difference is low. In that case, the obstructed segment could have been resolved by the treatment, but a new one may have appeared. Therefore, no conclusion can be drawn, and the metric needs to be tested with a larger study population.

Regarding the metric and results of the present work, it needs to be noted that quantitative volumetric data of both ventilation and perfusion scans were not evaluated in any of the referenced studies [10–17]. The main image analysis method is a qualitative assessment of the perfusion SPECT and segmental or subsegmental defects, as defined in the clinical guidelines of the EANM [3]. For example, Johns et al. [10] determined a positive or negative diagnosis for CTEPH based on visual interpretation of perfusion SPECT images. Wang et al. [15] also classified the images visually as positive or negative for PE, as the clinical guidelines do not differentiate between acute PE and CTEPH. In Renapurkar et al. [11], the defects in the perfusion SPECT scan are graded on a four-point scale and only planar V/Q scanning is used for quantitative measurements. On the other hand, Derlin et al. [17] studied the correlation between the perfusion volume and clinical parameters, but did not include the ventilation information nor conduct a classification procedure based on SPECT images. However, they showed that the perfusion volume is capable of identifying patients with mean PAP greater than 50 mmHg, which is a biomarker of PH (sensitivity, 80%; specificity, 64%).

Lastly, the implemented image segmentation algorithm requires further optimization. Thus, preprocessing should be added to remove possible tracer accumulations on the images. Moreover, alternative automatic segmentation algorithms like active contours could improve the detection of the perfused tissue. Computed tomography scans and its anatomical reference are also a useful tool for the quantitative analysis in CTEPH, as proposed in [17]. However, these were not available for the study group.

## 5. Conclusions

CTEPH is a severe variant of pulmonary hypertension and caused by the chronic occlusion of the pulmonary arteries by organized blood clots. It is currently diagnosed by the visual inspection of SPECT ventilation and perfusion images. A novel quantitative metric is proposed for the diagnosis of CTEPH, its differentiation from respiratory pathologies, and the evaluation of its treatment response. The difference of ventilation and perfusion volumes extracted from SPECT images is shown to be a viable option when analyzing SPECT V/Q images. Moreover, a quantitative scale, based on the analysis of a reference group of cases with similar ventilation and perfusion volumes, is defined for the automatic classification of new cases. The results show that the quantitative analysis of SPECT ventilation and perfusion images in patients with CTEPH could complement the visual analysis performed in clinical practice.

**Author Contributions:** Conceptualization, A.P.S., A.G.-G., P.P., P.C., H.B., J.E., E.J.G., and P.S.-G.; Data curation, A.P.S., A.G.-G., P.P., and P.C.; Formal analysis, A.P.S. and P.C.; Investigation, A.P.S., A.G.-G., P.P., P.C., H.B., J.E., E.J.G., and P.S.-G.; Methodology, A.P.S., A.G.-G., P.P., P.C., and P.S.-G.; Resources, A.G.-G., P.P., H.B., J.E., and E.J.G.; Software, A.P.S. and P.C.; Supervision, P.S.-G.; Validation, A.P.S., A.G.-G., P.P., P.C., and P.S.-G.; Visualization, A.P.S., P.C., and P.S.-G.; Writing—original draft, A.P.S., P.C., and P.S.-G.; Writing—review and editing, A.P.S., A.G.-G., P.P., P.C., H.B., J.E., E.J.G., and P.S.-G. All authors have read and agreed to the published version of the manuscript.

**Funding:** This research received no external funding.

**Acknowledgments:** The author A.P.S. received financial support through an FPU Fellowship (*Beca de Formación de Profesorado Universitario*) from the Spanish Ministry of Science, Innovation and Universities (FPU16/06487).

**Conflicts of Interest:** The authors declare no conflict of interest.

## References

1. Hoepfer, M.M.; Bogaard, H.J.; Condliffe, R.; Frantz, R.; Khanna, D.; Kurzyna, M.; Langleben, D.; Manes, A.; Satoh, T.; Torres, F.; et al. Definitions and Diagnosis of Pulmonary Hypertension. *J. Am. Coll. Cardiol.* **2013**, *62*, D42–D50. [[CrossRef](#)] [[PubMed](#)]
2. D'Alonzo, G.E.; Barst, R.J.; Ayres, S.M.; Bergofsky, E.H.; Brundage, B.H.; Detre, K.M.; Fishman, A.P.; Goldring, R.M.; Groves, B.M.; Kernis, J.T. Survival in Patients with Primary Pulmonary Hypertension. *Ann. Intern. Med.* **1991**, *115*, 343–349. [[CrossRef](#)] [[PubMed](#)]
3. Bajc, M.; Neilly, J.B.; Miniati, M.; Schuemichen, C.; Meignan, M.; Jonson, B. EANM guidelines for ventilation/perfusion scintigraphy: Part 1. Pulmonary imaging with ventilation/perfusion single photon emission tomography. *Eur. J. Nucl. Med. Mol. Imaging* **2009**, *36*, 1356–1370. [[CrossRef](#)] [[PubMed](#)]
4. Lang, I.M. Chronic thromboembolic pulmonary hypertension—Not so rare after all. *N. Engl. J. Med.* **2004**, *350*, 2236–2238. [[CrossRef](#)] [[PubMed](#)]
5. Tapsos, V.F.; Humbert, M. Incidence and prevalence of chronic thromboembolic pulmonary hypertension: From acute to chronic pulmonary embolism. *Proc. Am. Thorac. Soc.* **2006**, *3*, 564–567. [[CrossRef](#)] [[PubMed](#)]
6. Galiè, N.; Humbert, M.; Vachiery, J.-L.; Gibbs, S.; Lang, I.; Torbicki, A.; Simonneau, G.; Peacock, A.; Vonk Noordegraaf, A.; Beghetti, M.; et al. 2015 ESC/ERS Guidelines for the diagnosis and treatment of pulmonary hypertension. *Eur. Heart J.* **2016**, *37*, 67–119. [[CrossRef](#)] [[PubMed](#)]
7. Pepke-Zaba, J.; Ghofrani, H.A.; Hoepfer, M.M. Medical management of chronic thromboembolic pulmonary hypertension. *Eur. Respir. Rev.* **2017**, *26*, 160112. [[CrossRef](#)] [[PubMed](#)]
8. Anand, V.; Frantz, R.P.; DuBrock, H.; Kane, G.C.; Krowka, M.; Yanagisawa, R.; Sandhu, G.S. Balloon Pulmonary Angioplasty for Chronic Thromboembolic Pulmonary Hypertension: Initial Single-Center Experience. *Mayo Clin. Proc. Innov. Qual. Outcomes* **2019**, *3*, 311–318. [[CrossRef](#)] [[PubMed](#)]
9. Hoepfer, M.M.; Madani, M.M.; Nakanishi, N.; Meyer, B.; Cebotari, S.; Rubin, L.J. Chronic thromboembolic pulmonary hypertension. *Lancet Respir. Med.* **2014**, *2*, 573–582. [[CrossRef](#)]
10. Johns, C.S.; Swift, A.J.; Rajaram, S.; Hughes, P.J.C.; Capener, D.J.; Kiely, D.G.; Wild, J.M. Lung perfusion: MRI vs. SPECT for screening in suspected chronic thromboembolic pulmonary hypertension. *J. Magn. Reson. Imaging* **2017**, *46*, 1693–1697. [[CrossRef](#)] [[PubMed](#)]

11. Renapurkar, R.D.; Bolen, M.A.; Shrikanthan, S.; Bullen, J.; Karim, W.; Primak, A.; Heresi, G.A. Comparative assessment of qualitative and quantitative perfusion with dual-energy CT and planar and SPECT-CT V/Q scanning in patients with chronic thromboembolic pulmonary hypertension. *Cardiovasc. Diagn. Ther.* **2018**, *8*, 414–422. [[CrossRef](#)] [[PubMed](#)]
12. Koike, H.; Sueyoshi, E.; Sakamoto, I.; Uetani, M.; Nakata, T.; Maemura, K. Comparative clinical and predictive value of lung perfusion blood volume CT, lung perfusion SPECT and catheter pulmonary angiography images in patients with chronic thromboembolic pulmonary hypertension before and after balloon pulmonary angioplasty. *Eur. Radiol.* **2018**, *28*, 5091–5099. [[CrossRef](#)] [[PubMed](#)]
13. Koike, H.; Sueyoshi, E.; Sakamoto, I.; Uetani, M.; Nakata, T.; Maemura, K. Correlation between lung perfusion blood volume and SPECT images in patients with chronic thromboembolic pulmonary hypertension by balloon pulmonary angioplasty. *Clin. Imaging* **2018**, *49*, 80–86. [[CrossRef](#)] [[PubMed](#)]
14. Lasch, F.; Karch, A.; Koch, A.; Derlin, T.; Voskrebenev, A.; Alsady, T.M.; Hoepfer, M.M.; Gall, H.; Roller, F.; Harth, S.; et al. Comparison of MRI and VQ-SPECT as a Screening Test for Patients With Suspected CTEPH: CHANGE-MRI Study Design and Rationale. *Front. Cardiovasc. Med.* **2020**, *7*, 51. [[CrossRef](#)] [[PubMed](#)]
15. Wang, L.; Wang, M.; Yang, T.; Wu, D.; Xiong, C.; Fang, W. A Prospective, Comparative Study of Planar and Single-photon Emission Computed Tomography Ventilation/Perfusion Imaging for Chronic Thromboembolic Pulmonary Hypertension. *J. Nucl. Med.* **2020**. [[CrossRef](#)] [[PubMed](#)]
16. Wang, M.; Wu, D.; Ma, R.; Zhang, Z.; Zhang, H.; Han, K.; Xiong, C.; Wang, L.; Fang, W. Comparison of V/Q SPECT and CT Angiography for the Diagnosis of Chronic Thromboembolic Pulmonary Hypertension. *Radiology* **2020**, *296*, 420–429. [[CrossRef](#)]
17. Derlin, T.; Kelting, C.; Hueper, K.; Weiberg, D.; Meyer, K.; Olsson, K.M.; Thackeray, J.T.; Welte, T.; Bengel, F.M.; Hoepfer, M.M. Quantitation of Perfused Lung Volume Using Hybrid SPECT/CT Allows Refining the Assessment of Lung Perfusion and Estimating Disease Extent in Chronic Thromboembolic Pulmonary Hypertension. *Clin. Nucl. Med.* **2018**, *43*, e170–e177. [[CrossRef](#)] [[PubMed](#)]
18. Tsai, J.-Z.; Chang, M.-L.; Yang, J.-Y.; Kuo, D.; Lin, C.-H.; Kuo, C.-D. Left–Right Asymmetry in Spectral Characteristics of Lung Sounds Detected Using a Dual-Channel Auscultation System in Healthy Young Adults. *Sensors* **2017**, *17*, 1323. [[CrossRef](#)] [[PubMed](#)]
19. Soler, X.; Hoh, C.K.; Test, V.J.; Kerr, K.M.; Marsh, J.J.; Morris, T.A. Single photon emission computed tomography in chronic thromboembolic pulmonary hypertension. *Respirology* **2011**, *16*, 131–137. [[CrossRef](#)] [[PubMed](#)]
20. LoMauro, A.; Aliverti, A. Sex differences in respiratory function. *Breathe* **2018**, *14*, 131–140. [[CrossRef](#)] [[PubMed](#)]

